

## Theoretical Designs for Neutral Five-Membered Carbene Analogues of the Group 13 Elements: A New Target for Synthesis

Chi-Hui Chen and Ming-Der Su\*

Department of Applied Chemistry, National Chiayi University, Chiayi 60004, Taiwan

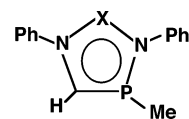
Received May 18, 2006

Potential energy surfaces for the chemical reactions of neutral five-membered group 13 carbenoids have been studied using density functional theory (B3LYP/LANL2DZ). Five five-membered group 13 carbenoid species,  $\text{HCMeP}(\text{PhN})_2\text{X}$ , where  $\text{X} = \text{B}, \text{Al}, \text{Ga}, \text{In}, \text{and Tl}$ , have been chosen as model reactants in this work. Also, three kinds of chemical reaction, C–H bond insertion, alkene cycloaddition, and dimerization, have been used to study the chemical reactivities of these group 13 carbenoids. Our present theoretical work predicts that the larger the  $\angle\text{NXN}$  bond angle in the neutral five-membered group 13 carbenoid, the smaller the singlet–triplet splitting, the lower the activation barrier, and, in turn, the more rapid are its various chemical reactions. Moreover, the theoretical investigations suggest that the relative carbenoid reactivity decreases in the order  $\text{B} > \text{Al} > \text{Ga} > \text{In} > \text{Tl}$ . That is, the heavier the group 13 atom (X), the more stable is its carbenoid with respect to chemical reactions. As a result, we predict that the neutral five-membered group 13 carbenoids ( $\text{X} = \text{Al}, \text{Ga}, \text{In}, \text{and Tl}$ ) should be stable, readily synthesized, and isolated at room temperature. Furthermore, the neutral five-membered group 13 carbenoid singlet–triplet energy splitting, as described in the configuration mixing model attributed to the work of Pross and Shaik, can be used as a diagnostic tool to predict their reactivities. The results obtained allow a number of predictions to be made.

## I. Introduction

The search for stable group 13 species<sup>1–4</sup> that are formally analogous to singlet carbenes<sup>5</sup> has aroused increasing interest in recent years because such compounds can show great potential as ligands in synthetic and coordination chemistry.<sup>6</sup> Much of the work in this area has centered on the neutral six-membered heterocycles that contain a group 13 metal in the +0 oxidation state.<sup>1–4</sup> On the other hand, only one species

containing anionic five-membered gallium(I), which is a valence isoelectronic N-heterocyclic carbene (NHC) analogue, has been structurally characterized to date.<sup>7</sup> As expected, however, this compound is very nucleophilic because of its anionic nature. Although many neutral six-membered heterocycles containing group 13 elements have now been investigated,<sup>1–4,6</sup> little is yet known about their neutral five-membered heterocyclic chemistry.<sup>8</sup>



X = B, Al, Ga, In, Tl

1

It is these fascinating experimental results<sup>1–4</sup> that inspire this study. If neutral six-membered group 13 carbenoid molecules can be chemically synthesized as stable com-

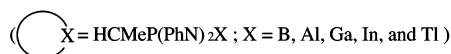
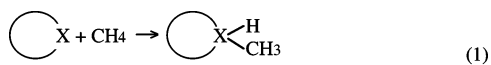
\* To whom correspondence should be addressed. E-mail: midesu@mail.ncyu.edu.tw.

- (1) For the divalent aluminum compounds, see: (a) Cui, C.; Roesky, H. W.; Schmidt, H.-G.; Noltemeyer, M.; Hao, H.; Cimpoesu, F. *Angew. Chem., Int. Ed.* **2000**, *39*, 4272. (b) Rao, M. N. S.; Roesky, H. W.; Anantharaman, G. *J. Organomet. Chem.* **2002**, *646*, 4.
- (2) For the divalent gallium compounds, see: (a) Hardman, N. J.; Eichler, B. E.; Power, P. P. *Chem. Commun.* **2000**, 1991. (b) Hardman, N. J.; Philips, A. D.; Power, P. P. *ACS Symp. Ser.* **2002**, *822*, 2. (c) Schmidt, E. S.; Jockisch, A.; Schmidbaur, H. *J. Am. Chem. Soc.* **1999**, *121*, 9758. (d) Baker, R. J.; Farley, R. D.; Jones, C.; Kloth, M.; Murphy, D. M. *J. Chem. Soc., Dalton Trans.* **2002**, 3844.
- (3) For the divalent indium compounds, see: (a) Hill, M. S.; Hitchcock, P. B. *Chem. Commun.* **2004**, 1818. (b) Hill, M. S.; Hitchcock, P. B.; Pongtavornpinyo, R. *J. Chem. Soc., Dalton Trans.* **2005**, 273.
- (4) For the divalent thallium compounds, see: (a) Cheng, Y.; Hitchcock, P. B.; Lappert, M. F.; Zhou, M. *Chem. Commun.* **2005**, 752. (b) ref 3b.
- (5) For reviews, see: (a) Driess, M.; Grutzmacher, H. *Angew. Chem., Int. Ed.* **1996**, *35*, 829. (b) Power, P. P. *J. Chem. Soc., Dalton Trans.* **1998**, 2939. (c) Power, P. P. *Chem. Rev.* **1999**, *99*, 3463.

- (6) For reviews, see: (a) Gemel, C.; Steinke, T.; Cokoja, M.; Kemper, A.; Fischer, R. A. *Eur. J. Inorg. Chem.* **2004**, 4161. (b) Baker, R. J.; Jones, C. *Coord. Chem. Rev.* **2005**, *249*, 1857.
- (7) Schmidt, E. S.; Jockisch, A.; Schmidbaur, H. *J. Am. Chem. Soc.* **1999**, *121*, 9758.

pounds, is it possible to extend syntheses to include other neutral five-membered group 13 carbenoid analogues? In this theoretical work, five neutral group 13 carbenoid analogues with six  $\pi$ -electrons (**1**) were selected as model systems for investigation of their various reaction. As far as we know, until now neither experimental nor theoretical studies have been performed on these systems. Our purpose here is (1) to find potential five-membered group 13 carbenoid analogues that can be stabilized, (2) to predict trends in activation energies and reaction enthalpies, (3) to obtain a better understanding of the origin of barrier heights for such chemical reactions, and (4) to provide experimentalists with a theoretical basis for predicting the relative reactivities of neutral five-membered group 13 carbenoid analogues.

Three kinds of chemical reactions are therefore discussed in this work. They are insertion, cycloaddition, and dimerization. These reactions have been chosen because they represent various possible neutral group 13 carbenoid reactions that have already been investigated extensively in the corresponding group 14 systems.<sup>9</sup> We thus present a density functional theory (DFT) study to investigate the potential energy surfaces and mechanisms of the following reactions:



That is, we consider theoretically the reaction paths of three kinds of model reactions involving a series of neutral group 13 carbenoids of the type HCMeP(PhN)<sub>2</sub>X, where X = B, Al, Ga, In, and Tl. Each of these pathways was examined computationally, and each is described in detail below. In fact, it should be pointed out that comparative studies are very useful in understanding similarities and differences in the chemical properties of molecules. It will be shown that the HCMeP(PhN)<sub>2</sub> ligand is very suitable for stabilization of neutral five-membered carbene homologues with higher elements of group 13 (X = Al, Ga, In, and Tl). Moreover, it is believed that, in view of recent dramatic developments in group 13 heavy-carbene chemistry,<sup>1–4,6,10</sup> analogous extensive studies of group 13 carbenoids should soon be forthcoming and will open up new areas.<sup>11</sup>

## II. Theoretical Methods

All geometries were fully optimized without imposing any symmetry constraints, although in some instances the resulting structure showed various elements of symmetry. For our DFT calculations,

(8) For related theoretical studies on a five-membered Arduengo-type carbene with a group 13 metal(I), see: (a) Sundermann, A.; Reiher, M.; Schoeller, W. W. *Eur. J. Inorg. Chem.* **1998**, 305. (b) Schoeller, W. W.; Eisner, D. *Inorg. Chem.* **2004**, *43*, 2585.

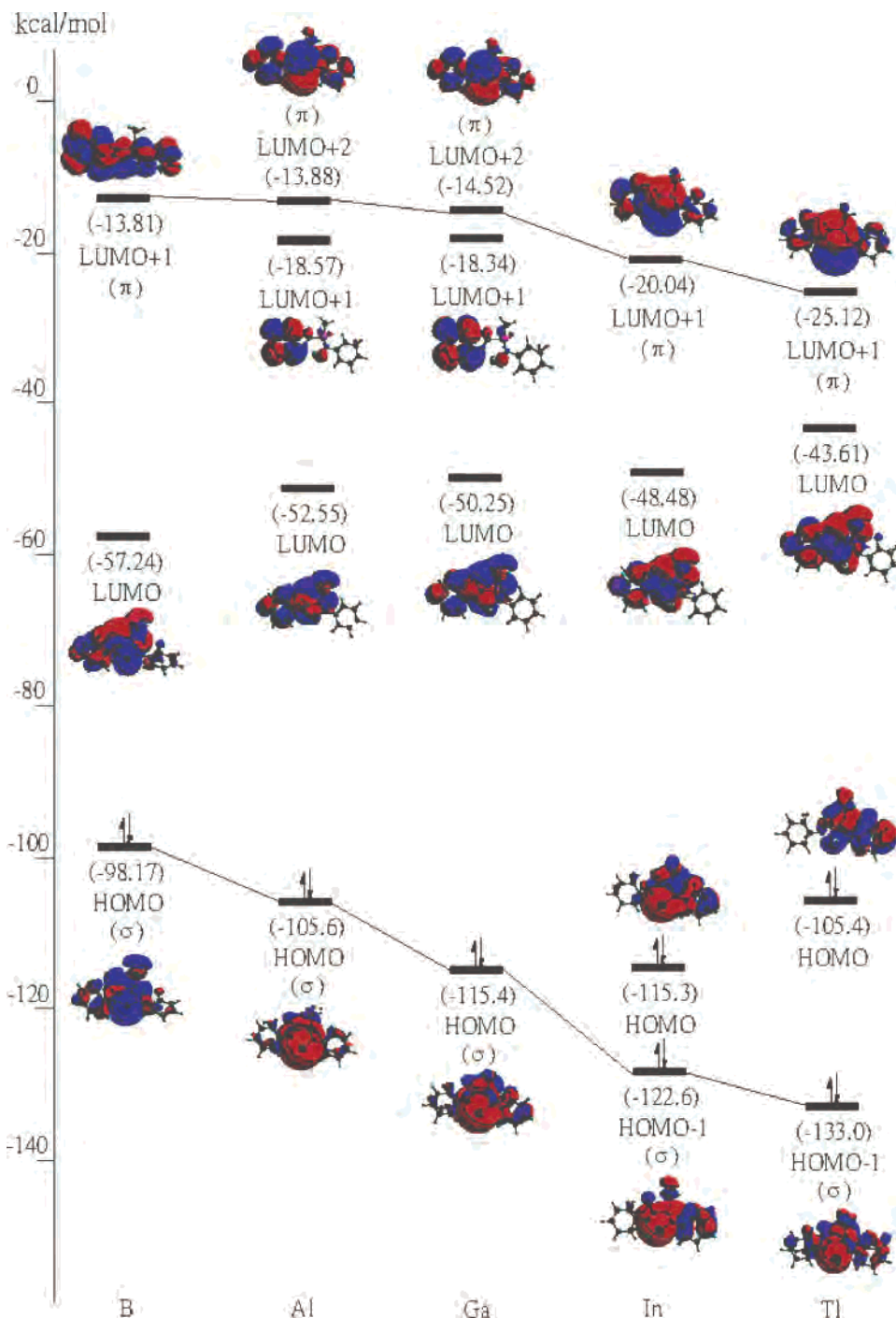
(9) For instance, see: (a) Su, M.-D.; Chu, S.-Y. *Chem. Phys. Lett.* **1999**, *308*, 283. (b) Su, M.-D.; Chu, S.-Y. *Inorg. Chem.* **1999**, *38*, 4819. (c) Su, M.-D.; Chu, S.-Y. *Chem. Phys. Lett.* **2000**, *320*, 475. (d) Su, M.-D. In *Leading Edge in Organometallic Chemistry Research*; Cato, M. A., Ed.; Nova Science Publishers: New York, 2006; Chapter 7. (e) Chen, C.-H.; Tsai, M.-L.; Su, M.-D. *Organometallics* **2006**, *25*, 2766.

we used the hybrid gradient-corrected exchange functional proposed by Becke,<sup>12</sup> combined with the gradient-corrected correlation functional of Lee, Yang, and Parr.<sup>13</sup> This functional is commonly known as B3LYP and has been shown to be quite reliable both for geometries and energies.<sup>14</sup> These B3LYP calculations were carried out with relativistic effective core potentials on group 13 elements modeled using the double- $\zeta$  (DZ) basis sets<sup>15</sup> augmented by a set of d-type polarization functions.<sup>15e</sup> Accordingly, we denote our B3LYP calculations by B3LYP/LANL2DZ. The spin-unrestricted (UB3LYP) formalism was used for the open-shell (triplet) species. The  $S^2$  expectation values of the triplet state for the open-shell reactants all showed an ideal value (2.00) after spin annihilation; therefore, their geometries and energetics are reliable for this study. Vibrational frequency calculations at the B3LYP/LANL2DZ level were used to characterize all stationary points as either minima (the number of imaginary frequencies (NIMAG) = 0) or transition states (NIMAG = 1). The relative energies were thus corrected for vibrational zero-point energies (ZPE, not scaled). Thermodynamic corrections to 298 K, ZPE corrections, heat capacity corrections, and entropy corrections ( $\Delta S$ ) were applied at the B3LYP/LANL2DZ level. Thus, the relative free energy ( $\Delta G$ ) at 298 K was also calculated at the same level of theory. All of the DFT calculations were performed using the GAUSSIAN 03 package of programs.<sup>16,17</sup>

## III. Results and Discussion

**(1) Geometries and Electronic Structures of HCMeP(PhN)<sub>2</sub>X.** To highlight the questions which form the basis for our study, it is worthwhile to first examine the geometries and electronic structures of the reactants (i.e., HCMeP(PhN)<sub>2</sub>X, whose valence molecular orbitals based on the

- (10) For the most recent reviews, see: (a) Weidenbruch, M. *Eur. J. Inorg. Chem.* **1999**, 373. (b) Haaf, M.; Schmedake, T. A.; West, R. *Inorg. Chem. Res.* **2000**, *33*, 704. (c) Gehrhuis, B.; Lappert, M. F. *J. Organomet. Chem.* **2001**, *617–618*, 209. (d) Hill, N. J.; West, R. *J. Organomet. Chem.* **2004**, *689*, 4165. (e) Kira, M. *J. Organomet. Chem.* **2004**, *689*, 4475. (f) Alder, R. W.; Blake, M. E.; Chaker, L. Harvey, J. N.; Paolini, F.; Schutz, J. *Angew. Chem. Int. Ed.* **2004**, *43*, 5896.
- (11) (a) Jones, C.; Junk, P. C.; Platts, J. A.; Stasch, A. *J. Am. Chem. Soc.* **2006**, *128*, 2206. (b) Jones, C.; Junk, P. C.; Platts, J. A.; Rathmann, D.; Stasch, A. *J. Chem. Soc., Dalton Trans.* **2005**, 2497.
- (12) (a) Becke, A. D. *Phys. Rev. A.* **1988**, *38*, 3098. (b) Becke, A. D. *J. Chem. Phys.* **1993**, *98*, 5648.
- (13) Lee, C.; Yang, W.; Parr, R. G. *Phys. Rev. B* **1988**, *37*, 785.
- (14) (a) Su, M.-D. *J. Phys. Chem. A* **2004**, *108*, 823. (b) Su, M.-D. *Inorg. Chem.* **2004**, *43*, 4846. (c) Su, M.-D. *Eur. J. Chem.* **2005**, *10*, 5877 and references therein.
- (15) (a) Dunning, T. H., Jr.; Hay, P. J. In *Modern Theoretical Chemistry*; Schaefer, H. F., III, Ed.; Plenum: New York, 1976; pp 1–28. (b) Hay, P. J.; Wadt, W. R. *J. Chem. Phys.* **1985**, *82*, 270. (c) Hay, P. J.; Wadt, W. R. *J. Chem. Phys.* **1985**, *82*, 284. (d) Hay, P. J.; Wadt, W. R. *J. Chem. Phys.* **1985**, *82*, 299. (e) Höllwarth, A.; Böhme, M.; Dapprich, S.; Ehlers, A. W.; Gobbi, A.; Jonas, V.; Köhler, K. F.; Stegmann, R.; Veldkamp, A.; Frenking, G. *Chem. Phys. Lett.* **1993**, *208*, 237.
- (16) Frisch, M. J.; Trucks, G. W.; Schlegel, H. B.; Scuseria, G. E.; Robb, M. A.; Cheeseman, J. R.; Zakrzewski, V. G.; Montgomery, J. A., Jr.; Vreven, T.; Kudin, K. N.; Burant, J. C.; Millam, J. M.; Iyengar, S. S.; Tomasi, J.; Barone, V.; Mennucci, B.; Cossi, M.; Scalmani, G.; Rega, N.; Petersson, G. A.; Nakatsuji, H.; Hada, M.; Ehara, M.; Toyota, K.; Fukuda, R.; Hasegawa, J.; Ishida, M.; Nakajima, T.; Honda, Y.; Kitao, O.; Nakai, H.; Klene, M.; Li, X.; Knox, J. E.; Hratchian, H. P.; Cross, J. B.; Adamo, C.; Jaramillo, J.; Gomperts, R.; Stratmann, R. E.; Yazyev, O.; Austin, A. J.; Cammi, R.; Pomelli, C.; Ochterski, J. W.; Ayala, P. Y.; Morokuma, K.; Voth, G. A.; Salvador, P.; Dannenberg, J. J.; Zakrzewski, V. G.; Dapprich, S.; Daniels, A. D.; Strain, M. C.; Farkas, O.; Malick, D. K.; Rabuck, A. D.; Raghavachari, K.; Foresman, J. B.; Ortiz, J. V.; Cui, Q.; Baboul, A. G.; Clifford, S.; Cioslowski, J.; Stefanov, B. B.; Liu, G.; Liashenko, A.; Piskorz, P.; Komaromi, I.; Martin, R. L.; Fox, D. J.; Keith, T.; Al-Laham, M. A.; Peng, C. Y.; Nanayakkara, A.; Challacombe, M.; Gill, P. M. W.; Johnson, B.; Chen, W.; Wong, M. W.; Gonzalez, C.; Pople, J. A. *Gaussian 03*; Gaussian, Inc.: Wallingford, CT, 2003.

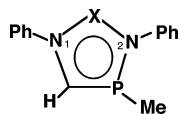


**Figure 1.** Calculated frontier molecular orbital for the HCMeP(PhN)<sub>2</sub>X (X = B, Al, Ga, In, and Tl) species. For more information see the text.

B3LYP/LANL2DZ calculations are presented in Figure 1). The optimized geometries for these neutral five-membered group 13 carbenoids calculated at the B3LYP/LANL2DZ level of theory and their selected geometrical parameters are collected in Table 1. Their Cartesian coordinates are included in the Supporting Information.

As one can see in Figure 1, the substitution of a single X atom at the HCMeP(PhN)<sub>2</sub>X center decreases the energy of the  $\sigma$  orbital on going from B to Tl (i.e.,  $E\sigma(\text{B}) > E\sigma(\text{Al}) > E\sigma(\text{Ga}) > E\sigma(\text{In}) > E\sigma(\text{Tl})$ ). Similarly, this substitution also decreases the p- $\pi$  orbital energy down group 13 (i.e.,  $E_{p-\pi}(\text{B}) > E_{p-\pi}(\text{Al}) > E_{p-\pi}(\text{Ga}) > E_{p-\pi}(\text{In}) > E_{p-\pi}(\text{Tl})$ ).

These two effects combined lead to an increased HOMO-LUMO energy difference for the HCMeP(PhN)<sub>2</sub>X reactant in the heavier group 13 species (vide infra). However, it should be noted that the nature of the HOMO and the LUMO in HCMeP(PhN)<sub>2</sub>X, especially for X = In and Tl, is quite different from that encountered in most group 14 divalent compounds.<sup>18</sup> Here, the HOMO of HCMeP(PhN)<sub>2</sub>X (X = B, Al, and Ga) is essentially a nonbonding  $\sigma$  orbital. This lone-pair orbital is arranged in the cyclic plane of the HCMeP(PhN)<sub>2</sub>X species in a pseudotrigonal planar fashion with respect to the two sets of X-N linkages. As a result, such lone pairs can be viewed as being located within an

**Table 1.** Selected Geometric Values and Relative Energies for Singlet and Triplet Group 13 Carbenoids, HCMeP(PhN)<sub>2</sub>X, where X = B, Al, Ga, In, and Tl<sup>a,b</sup>

system	X = B	X = Al	X = Ga	X = In	X = Tl
	singlet				
X–N1 (Å)	1.485	2.222	2.312	2.471	2.662
X–N2 (Å)	1.416	1.928	1.966	2.146	2.398
N1–C (Å)	1.371	1.306	1.302	1.303	1.301
N2–P (Å)	1.904	1.791	1.791	1.784	1.780
∠NXN (deg)	111.7	83.56	82.08	78.02	73.73
	triplet				
X–N1 (Å)	1.449	1.875	1.894	2.085	2.444
X–N2 (Å)	1.415	1.837	1.853	2.049	2.637
N1–C (Å)	1.415	1.401	1.398	1.390	1.378
N2–P (Å)	1.877	1.842	1.838	1.824	1.860
∠NXN (deg)	115.3	98.21	97.69	90.80	75.86
ΔE <sub>st</sub> (kcal mol <sup>-1</sup> )	-12.90	16.22	24.50	32.48	34.69

<sup>a</sup> All calculations were performed at the B3LYP/LANL2DZ (singlet) and UB3LYP/LANL2DZ (triplet) levels of theory. <sup>b</sup> Energy relative to the corresponding singlet state. A positive value means the singlet is the ground state.

orbital of predominant sp character. It should therefore be noted that the existence of a nonbonded lone pair of electrons at the X center strongly endorses the singlet carbene character of the neutral group 13 carbenoids (vide infra). In addition, the reason that the indium and thallium lone pair ( $\sigma$ ) orbitals (HOMO–1) are located below their HOMOs may be attributed to the “orbital nonhybridization effect”, also known as the “inert s-pair effect”.<sup>19</sup> This would make the valence s orbital more strongly contracted than the corresponding p orbitals. In turn, the size difference between the valence s and p orbitals increases from B to Tl. Consequently, it tends to form a nonbonding orbital acquiring mainly s character, whereas the remaining p electrons are used to form  $\pi$  bonds with the neighboring heavy atom. Moreover, such phenomena can also be found in the LUMO of heavy HCMeP(PhN)<sub>2</sub>X compounds. As can be seen in Figure 1, our present theoretical results indicate that the LUMO in each case is entirely ligand-based and of  $\pi$  symmetry. Indeed, the valence unoccupied orbital of HCMeP(PhN)<sub>2</sub>X corresponding to the X p– $\pi$  orbital would be the LUMO+1 (X = B, In, and Tl) or the LUMO+2 (X = Al and Ga) level. Accordingly, these effects cause the energy gap for the neutral five-membered group 13 carbenoids to increase in the order B < Al < Ga < In < Tl (vide infra).

The HCMeP(PhN)<sub>2</sub>X compounds have been calculated both as spin-paired (singlet state) and as spin-unpaired (triplet state) molecules. As one can see in Table 1, regardless of multiplicity, both the X–N1 and X–N2 bond lengths show a monotonic increase from X = B to Tl. For instance, both the X–N1 and X–N2 distances increase in the order X = B (1.485 and 1.416 Å) < Al (2.222 and 1.928 Å) < Ga (2.312 and 1.965 Å) < In (2.471 and 2.146 Å) < Tl (2.662 and 2.398 Å). The same thing can be found in the triplet neutral group 13 carbenoids as shown in Table 1. Moreover, our theoretical investigations also point out that both X–N1 and X–N2 distances are larger for the singlet than for the equivalent triplet species, while the bond angle ∠NXN is smaller for the singlet than for its equivalent triplet. In addition, regardless of its multiplicity, the bond angle ∠NXN decreases uniformly as the central atom, X, is changed from B to Tl. Accordingly, it is apparent that, as the X atom becomes heavier, a more acute bond angle ∠NXN is favored. Again, the reason for this may be the relativistic effect<sup>18</sup> as discussed above.

Although one may identify the spin of the ground state by experiment (e.g., from ESR spectroscopy), it is quite difficult to experimentally determine the magnitude of the singlet–triplet splitting ( $\Delta E_{st} = E_{\text{triplet}} - E_{\text{singlet}}$ ). Fortunately, moderately sophisticated molecular orbital theory can provide a good estimate of the singlet–triplet splitting in these neutral five-membered group 13 carbenoids. As demonstrated in Table 1, the DFT results show that the values of  $\Delta E_{st}$  for boron, aluminum, gallium, indium, and thallium are –12.90, +16.22, +24.50, +32.48, and +34.69 kcal/mol, respectively (i.e.,  $\Delta E_{st}$  increases in the order B < Al < Ga < In < Tl). That is to say, the heavier group 13 atoms have larger singlet–triplet splitting. Again, these phenomena can be satisfactorily explained by the relativistic effect<sup>19</sup> as mentioned previously. In addition, it should be pointed out that the stabilities of these carbene analogues are determined by their singlet–triplet splitting. Namely, if  $\Delta E_{st}$  is small, the carbene-like structures will be unstable and will be capable of facile chemical reactions (such as with solvents, etc.).<sup>8</sup> It will be demonstrated below that the singlet–triplet splitting of the neutral five-membered group 13 carbenoids can be used as a guide to predict its reactivity.

Indeed, according to Su’s work<sup>18c</sup>, which is based on the theory of Pross and Shaik,<sup>20,21</sup> the singlet–triplet splitting of a carbene plays a crucial role in many chemical reactions (i.e., the relative stabilities of the lowest singlet and triplet states are in turn a sensitive function of the barrier height for carbenic reactivity). Since, as mentioned above, neutral five-membered group 13 carbenoids are analogues of CH<sub>2</sub>,

- (17) One referee pointed out that a single-point calculation with a large quality basis set on each of structures should be good for this kind of problem. We used the WTBS basis set (see *Chem. Phys. Lett.* **1993**, *212*, 260) based on the B3LYP level of theory to do the single-point calculations for each stationary point studied in this work. Our results, based on the B3LYP/LANL2DZ/B3LYP/WTBS method, are basically similar to those found on the B3LYP/LANL2DZ level of theory. We have made discussion on these molecular systems. See the Supporting Information.
- (18) (a) Su, M.-D.; Chu, S.-Y. *Inorg. Chem.* **1999**, *38*, 4819. (b) Su, M.-D. *J. Phys. Chem. A* **2002**, *106*, 9563. (c) Su, M.-D. *Inorg. Chem.* **1995**, *34*, 3829.
- (19) (a) Pykkö, P.; Desclaux, J.-P. *Acc. Chem. Res.* **1979**, *12*, 276. (b) Kutzelnigg, W. *Angew. Chem., Int. Ed. Engl.* **1984**, *23*, 272. (c) Pykkö, P. *Chem. Rev.* **1988**, *88*, 563. (d) Pykkö, P. *Chem. Rev.* **1997**, *97*, 597.

- (20) For details, see: (a) Shaik, S.; Schlegel, H. B.; Wolfe, S. In *Theoretical Aspects of Physical Organic Chemistry*; John Wiley & Sons Inc.: New York, 1992. (b) Pross, A. In *Theoretical and Physical Principles of Organic Reactivity*; John Wiley & Sons Inc.: New York, 1995. (c) Shaik, S. *Prog. Phys. Org. Chem.* **1985**, *15*, 197. (d) Shaik, S. In *Theory and Applications of Computational Chemistry*; Dykstra, C. E., Frenking, G., Kim, K. S., Scuseria, G. E., Eds.; Elsevier: New York, 2003.
- (21) (a) For the first paper that originated the CM model, see: Shaik, S. *J. Am. Chem. Soc.* **1981**, *103*, 3692. (b) For the most updated review of the CM model, see: Shaik, S.; Shurki, A. *Angew. Chem., Int. Ed. Engl.* **1999**, *38*, 586.

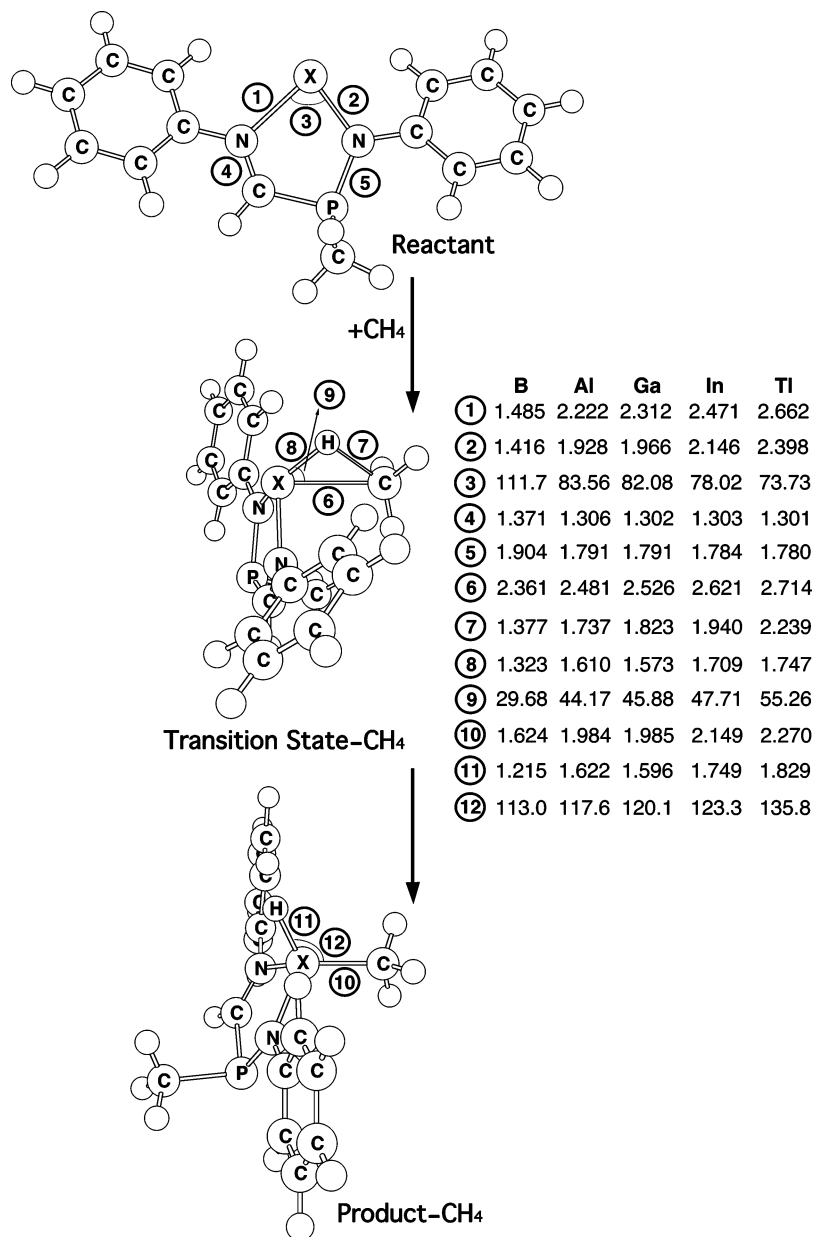


**Figure 2.** B3LYP/LANL2DZ-optimized geometries (in Å and deg) of the reactants (singlet), transition states, and insertion products of  $\text{HcMeP}(\text{PhN})_2\text{X}$  ( $\text{X} = \text{B}, \text{Al}, \text{Ga}, \text{In}, \text{and Tl}$ ) and  $\text{CH}_4$ . The relative energies for each species are given in Table 2. Hydrogens are omitted for clarity.

one may envision that these predictions for carbenic reactivity should also apply to the neutral five-membered group 13 systems. Moreover, our findings show that it is the size of this energy gap that in large part controls the chemical behavior of these chemical species. In fact, combining insights from the configuration-mixing (CM) model<sup>20,21</sup> and the previous bond-angle model predictions, one may therefore conclude that the larger the  $\angle\text{NXN}$  bond angle, the smaller  $\Delta E_{\text{st}}$ , the lower the barrier height, the greater the exothermicity, and in turn, the faster the chemical reactions.

Finally, as seen from Table 1, our DFT calculations demonstrate that the  $\text{HcMeP}(\text{PhN})_2\text{X}$  ( $\text{X} = \text{Al}, \text{Ga}, \text{In}, \text{and Tl}$ ) species possess a singlet ground state, except for the boron case.<sup>22</sup> This strongly implies that all three reactions (eq 1–3) should proceed on the singlet surface. We shall thus focus on the singlet surface from now on.

**(2) Geometries and Energetics of  $\text{HcMeP}(\text{PhN})_2\text{X} + \text{CH}_4$ .** We shall consider mechanisms which proceed via eq 1, focusing on the transition states as well as on the insertion products themselves. For convenience, the chemical reactions considered here are as follows: reactants (**Rea- $\text{CH}_4$** )  $\rightarrow$  transition state (**TS- $\text{CH}_4$** )  $\rightarrow$  insertion product (**Pro- $\text{CH}_4$** ). The optimized geometries calculated at the B3LYP/LANL2DZ level of theory involving **Rea- $\text{CH}_4$** , **TS- $\text{CH}_4$** , and **Pro- $\text{CH}_4$**  are collected in Figure 2. The corresponding energetics are summarized in Table 2. Cartesian coordinates calculated for the stationary points at the B3LYP level are available as

(22) However, as one can see in Table 1, the ground state of  $\text{HcMeP}(\text{PhN})_2\text{B}$  is the triplet state with the singlet–triplet splitting of  $-12.90$  kcal/mol. Nevertheless, for consistency, we still use the singlet state in all three reactions (eqs 1–3).

**Table 2.** Relative Energies for Singlet and Triplet Group 13 Carbenoids (HCMeP(PhN)<sub>2</sub>X) and for the CH<sub>4</sub> Insertion Process, Reactants (HCMeP(PhN)<sub>2</sub>X + CH<sub>4</sub>) → Transition State → Insertion Product<sup>a,b</sup>

system	$\Delta E_{\text{st}}^c$ (kcal mol <sup>-1</sup> )	$\angle \text{NXN}$ (deg)	$\Delta E_{\ddagger}^d$ (kcal mol <sup>-1</sup> )	$\Delta H^e$ (kcal mol <sup>-1</sup> )
X = B	-12.90	111.7	16.27	-47.18
X = Al	16.22	83.56	49.07	-22.04
X = Ga	24.50	82.08	56.92	-9.841
X = In	32.48	78.02	67.81	4.917
X = Tl	34.69	73.73	100.5	47.79

<sup>a</sup> All calculations were performed at the B3LYP/LANL2DZ level of theory. For the B3LYP optimized structures of the stationary points, see Figure 2. <sup>b</sup> Energies differences have been zero-point corrected. See the text. <sup>c</sup> Energy relative to the corresponding singlet state. A positive value means the singlet is the ground state. <sup>d</sup> The activation energy of the transition state, relative to the corresponding reactants. <sup>e</sup> The reaction enthalpy of the product, relative to the corresponding reactants.

Supporting Information. Figure 2 and Table 2 reveal some noteworthy features.

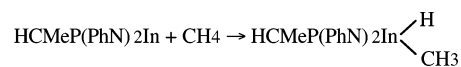
For the reaction path in eq 1, we have located the transition state (**TS-CH<sub>4</sub>**) for each neutral five-membered HCMeP(PhN)<sub>2</sub>X species at the B3LYP/LANL2DZ level of theory, along with the imaginary frequency eigenvector (see Figure 2 and Table 2). These reactions appear to be concerted; we have been able to locate only one TS for each reaction and have confirmed that it is a true transition state on the basis of frequency analysis. The B3LYP/LANL2DZ frequency calculations for the transition states **TS-B-CH<sub>4</sub>**, **TS-Al-CH<sub>4</sub>**, **TS-Ga-CH<sub>4</sub>**, **TS-In-CH<sub>4</sub>**, and **TS-Tl-CH<sub>4</sub>** suggest that the single imaginary frequency values are 1018i, 1204i, 1140i, 1088i, and 1068i cm<sup>-1</sup>, respectively. As shown in Figure 2, vibrational motion for the 1,2-hydrogen migration involves bond formation between the group 13 (X) atom and the carbon in concert with one C–H bond breaking. Moreover, our attempt to locate the abstraction transition states between the neutral five-membered HCMeP(PhN)<sub>2</sub>X species and methane failed. Thus, our theoretical investigations suggest that the addition reaction of neutral five-membered HCMeP(PhN)<sub>2</sub>X to CH<sub>4</sub> proceeds via a one-step process. That such addition reactions follow a concerted pathway is also supported by the geometries of the transition states as demonstrated in Figure 2.

A further detailed comparison of the five transition structures leads to the following remarks: for instance, as seen in Figure 2, all transition states are early, as shown by the large values of the newly breaking C–H bond length that ranges from 1.377 Å for the C–H bond length in **TS-B-CH<sub>4</sub>** to 2.239 Å for the C–H bond length in **TS-Tl-CH<sub>4</sub>**. Moreover, the newly formed C–X bond length increases in the following order: **TS-B-CH<sub>4</sub>** (2.361 Å) < **TS-Al-CH<sub>4</sub>** (2.481 Å) < **TS-Ga-CH<sub>4</sub>** (2.526 Å) < **TS-In-CH<sub>4</sub>** (2.621 Å) < **TS-Tl-CH<sub>4</sub>** (2.714 Å). Also, our B3LYP calculations show that the newly formed X–H bond length in these transition states increases in the order **TS-B-CH<sub>4</sub>** (1.323 Å) < **TS-Ga-CH<sub>4</sub>** (1.573 Å) < **TS-Al-CH<sub>4</sub>** (1.610 Å) < **TS-In-CH<sub>4</sub>** (1.709 Å) < **TS-Tl-CH<sub>4</sub>** (1.747 Å). Namely, the above structural features indicate that the transition structures for the insertion reaction of neutral five-membered group 13 carbenoids containing a more electronegative atom (X)

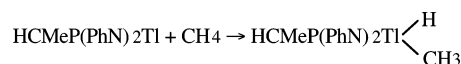
are more reactant-like. This is consistent with the Hammond postulate,<sup>23</sup> which associates an earlier transition state with a smaller reaction barrier and a larger exothermicity. As will be shown below, the insertion reaction of a neutral five-membered group 13 system with a more reactant-like transition structure does have a smaller activation barrier and a larger exothermicity.

The barrier heights predicted at the B3LYP/LANL2DZ level for these insertion reactions are given in Table 2. In accordance with the trends of the transition structures, the barrier heights for the insertion reactions of neutral five-membered group 13 carbenoids increase in the following order (kcal/mol): **TS-B-CH<sub>4</sub>** (16.27) < **TS-Al-CH<sub>4</sub>** (49.07) < **TS-Ga-CH<sub>4</sub>** (56.92) < **TS-In-CH<sub>4</sub>** (67.81) < **TS-Tl-CH<sub>4</sub>** (100.5). Thus, our calculations indicate that the more electronegative the atom involved in the insertion reaction, the lower the activation barrier for its insertion reaction.

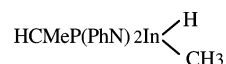
The neutral five-membered group 13 systems studied here produce five insertion products (i.e., **Pro-B-CH<sub>4</sub>**, **Pro-Al-CH<sub>4</sub>**, **Pro-Ga-CH<sub>4</sub>**, **Pro-In-CH<sub>4</sub>**, and **Pro-Tl-CH<sub>4</sub>**). The optimized geometries for these insertion products are also depicted in Figure 2. In these products, the newly formed intermolecular bond lengths (X–C and X–H bond) range from 1.624 and 1.215 Å in **Pro-B-CH<sub>4</sub>** to 2.270 and 1.829 Å in **Pro-Tl-CH<sub>4</sub>**. These bond lengths are typical for the X–C and X–H (X = B, Al, Ga, In, and Tl) single bonds and follow the same trend that the more electropositive the X atom, the longer the X–C and X–H bonds. Furthermore, as shown in Table 2, only three insertion reactions are thermodynamically exothermic (i.e., X = B, Al, and Ga), whereas the other two insertion reactions are thermodynamically endothermic (i.e., X = In and Tl). That is, the energies of **Pro-In-CH<sub>4</sub>** and **Pro-Tl-CH<sub>4</sub>** are above those of their corresponding starting materials. This strongly suggests that the insertion reactions into neutral five-membered indium and thallium systems are energetically unfavorable and would be endothermic. As Table 2 shows, the order of enthalpy follows the same trend as that of the activation energy (kcal/mol): **Pro-B-CH<sub>4</sub>** (–47.18) < **Pro-Al-CH<sub>4</sub>** (–22.04) < **Pro-Ga-CH<sub>4</sub>** (–9.841) < **Pro-In-CH<sub>4</sub>** (+4.917) < **Pro-Tl-CH<sub>4</sub>** (+47.79). Namely, our theoretical findings suggest that the insertion products of HCMeP(PhN)<sub>2</sub>In and HCMeP(PhN)<sub>2</sub>Tl are not produced from the methane insertion reactions of



and

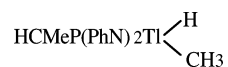


respectively, but possibly exist if these compounds,



(23) Hammond, G. S. *J. Am. Chem. Soc.* **1954**, *77*, 334.

and



are produced through other reaction paths.

Furthermore, as mentioned previously, the  $\angle\text{NXN}$  bond angle of a neutral five-membered group 13 carbenoid seems to parallel the same trend as the barrier height and reaction enthalpy for its insertion reaction with methane, as given in Table 2. Namely, the larger the  $\angle\text{NXN}$  bond angle of the neutral five-membered group 13 carbenoid, the smaller the singlet–triplet splitting and, in turn, the easier the insertion reaction. As a consequence, our model observations provide strong evidence that an electronic factor resulting from the bending of the  $\angle\text{NXN}$  bond as well as the singlet–triplet energy gap ( $\Delta E_{\text{st}}$ ) plays a decisive role in determining the reactivity of neutral five-membered group 13 carbenoids.<sup>24</sup>

**(3) Geometries and Energetics of HCMeP(PhN)<sub>2</sub>X + C<sub>2</sub>H<sub>4</sub>.** We next consider addition mechanisms which proceed via eq 2. For consistency with our previous work, the following reaction mechanism has been used to explore the cycloaddition reaction of a heterocyclic group 13 system to ethylene: reactants (**Rea-C<sub>2</sub>H<sub>4</sub>**) → transition state (**TS-C<sub>2</sub>H<sub>4</sub>**) → addition product (**Pro-C<sub>2</sub>H<sub>4</sub>**). For the systems (X = B, Al, Ga, In, and Tl), their geometries and energetics have been calculated using the B3LYP/LANL2DZ level of theory. The selected geometrical parameters and the relative energies of stationary points for the above mechanism are collected in Figure 3 and Table 3. Cartesian coordinates calculated for the stationary points at the B3LYP level are available as Supporting Information. The major conclusions drawn from the current study can be summarized as follows.

As predicted before, a neutral five-membered HCMeP(PhN)<sub>2</sub>X species and ethylene should undergo a [1+2] cycloaddition with a barrier to form a cycloaddition product. As one can see in Figure 3, it is evident that these transition states (i.e., **TS-B-C<sub>2</sub>H<sub>4</sub>**, **TS-Al-C<sub>2</sub>H<sub>4</sub>**, **TS-Ga-C<sub>2</sub>H<sub>4</sub>**, **TS-In-C<sub>2</sub>H<sub>4</sub>**, and **TS-Tl-C<sub>2</sub>H<sub>4</sub>**), which all are at the first-order saddle point as determined by the frequency calculations at the B3LYP/LANL2DZ level, proceed in a three-center pattern involving the group 13 and two carbon atoms. Our B3LYP/LANL2DZ frequency calculations for the transition states **TS-B-C<sub>2</sub>H<sub>4</sub>**, **TS-Al-C<sub>2</sub>H<sub>4</sub>**, **TS-Ga-C<sub>2</sub>H<sub>4</sub>**, **TS-In-C<sub>2</sub>H<sub>4</sub>**, and **TS-Tl-C<sub>2</sub>H<sub>4</sub>** indicate that the single imaginary frequency values are 112i, 176i, 177i, 130i, and 142i cm<sup>-1</sup>, respectively. Their normal modes associated with the single imaginary frequency are consistent with the C=C activation process, primarily the C=C bond stretching with a group 13 atom migrating to the double bond. It should be pointed out that such characteristic three-centered cyclic transition states are quite analogous to mechanisms observed for the addition reactions of singlet carbene.<sup>25,26</sup>

Moreover, our B3LYP/LANL2DZ results demonstrate that the larger the  $\angle\text{NXN}$  bond angle, the more reactant-like the transition state structure. From Figure 3, it is apparent that

the lengths of the C=C bond for **TS-B-C<sub>2</sub>H<sub>4</sub>**, **TS-Al-C<sub>2</sub>H<sub>4</sub>**, **TS-Ga-C<sub>2</sub>H<sub>4</sub>**, **TS-In-C<sub>2</sub>H<sub>4</sub>**, and **TS-Tl-C<sub>2</sub>H<sub>4</sub>** are 1.358, 1.441, 1.465, 1.502, and 1.602 Å, respectively, in comparison with free ethene (1.330 Å). In addition, one may easily see that the activation energy (kcal/mol) of the transition state follows the same trend as the singlet–triplet splitting of the neutral five-membered HCMeP(PhN)<sub>2</sub>X system (i.e., **TS-B-C<sub>2</sub>H<sub>4</sub>** (2.938) < **TS-Al-C<sub>2</sub>H<sub>4</sub>** (5.048) < **TS-Ga-C<sub>2</sub>H<sub>4</sub>** (14.61) < **TS-In-C<sub>2</sub>H<sub>4</sub>** (28.30) < **TS-Tl-C<sub>2</sub>H<sub>4</sub>** (75.18)). That is to say, according to the CM model,<sup>20,21</sup> one predicts that a neutral five-membered HCMeP(PhN)<sub>2</sub>X species with a more electronegative atom would have a larger  $\angle\text{NXN}$  bond angle, a smaller  $\Delta E_{\text{st}}$ , and a more facile cycloaddition to ethylene.

Finally, as one can see in Table 3, the energy of the final cycloproducts relative to their corresponding reactants are -48.51 (**Pro-B-C<sub>2</sub>H<sub>4</sub>**), -8.483 (**Pro-Al-C<sub>2</sub>H<sub>4</sub>**), +6.940 (**Pro-Ga-C<sub>2</sub>H<sub>4</sub>**), +25.70 (**Pro-In-C<sub>2</sub>H<sub>4</sub>**), and +75.10 kcal/mol (**Pro-Tl-C<sub>2</sub>H<sub>4</sub>**), indicating that the neutral five-membered HCMeP(PhN)<sub>2</sub>X molecule with a more electropositive group 13 atom (X) should be more endothermic. Also, it should be noted that the order of the reaction enthalpy seems to follow the same trend as the  $\angle\text{NXN}$  bond angle, as well as the singlet–triplet splitting ( $\Delta E_{\text{st}}$ ). In other words, our model calculations demonstrate that the values of  $\Delta E_{\text{st}}$  are remarkably diagnostic of the reactivities of neutral five-membered heterocyclic species.

**(4) Geometries and Electronic Structures of Dimerization Reactions.** To understand more information about the kinetic stability of the neutral five-membered HCMeP(PhN)<sub>2</sub>X molecule, its dimerization reaction was investigated in this work. Selected geometrical parameters for the stationary point structures along the pathway given in eq 3 and calculated at the B3LYP/LANL2DZ level are shown in Figure 4. The relative energies obtained at the same level of theory are collected in Table 4. Cartesian coordinates for these stationary points are included in the Supporting Information. There are several important conclusions from these results to which attention should be drawn.

As expected, a double bond between the two group 13 atoms should be formed during the dimerization reaction. Nevertheless, repeated attempts to find the transition state for a concerted dimerization of two HCMeP(PhN)<sub>2</sub>X species using the DFT methodology came to nothing. It was therefore concluded that no transition states exists on the B3LYP surface for such a dimerization. Furthermore, our thermodynamic results prove that all five dimers (i.e., **Pro-B-dimer**, **Pro-Al-dimer**, **Pro-Ga-dimer**, **Pro-In-dimer**, and **Pro-Tl-dimer**) contain no imaginary frequency and, in turn, can be considered as true minima on the B3LYP potential energy surfaces. As already shown in Figure 4, it is clear that the two monomer molecules were positioned with the two five-membered ring planes nearly orthogonal to each other because of the two bulky protecting groups around the group 13 center. Unfortunately, as we have mentioned earlier,

(24) Su, M.-D. *J. Chin. Chem. Soc.* **2005**, *52*, 599.

(25) (a) Hoffmann, R. *J. Am. Chem. Soc.* **1968**, *90*, 1475. (b) Zurawski, B.; Kutzelnigg, W. *J. Am. Chem. Soc.* **1978**, *100*, 2654. (c) Rondan, N. G.; Houk, K. N.; Moss, R. A. *J. Am. Chem. Soc.* **1980**, *102*, 1770. (26) Su, M.-D. *J. Phys. Chem.* **1996**, *100*, 4339 and references therein.

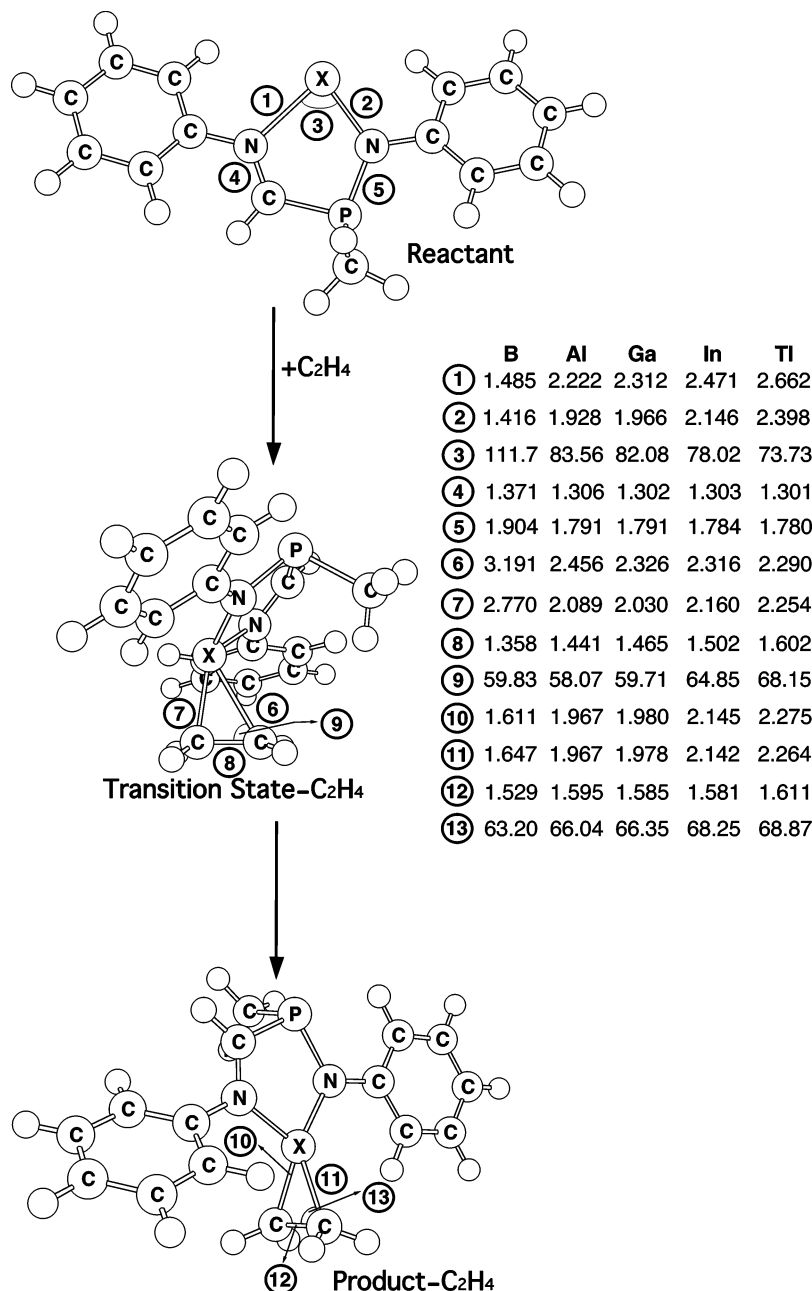


**Figure 3.** B3LYP/LANL2DZ-optimized geometries (in Å and deg) of the reactants (singlet), transition states, and addition products of  $\text{HCMeP}(\text{PhN})_2\text{X}$  ( $\text{X} = \text{B}, \text{Al}, \text{Ga}, \text{In}, \text{and Tl}$ ) and  $\text{C}_2\text{H}_4$ . The relative energies for each species are given Table 3. Hydrogens are omitted for clarity.

because of a lack of experimental and theoretical data on such bonded species, the geometrical values presented in this work should be considered as predictions for future investigations.

Our B3LYP computations indicate that the greater the atomic number of the group 13 element, the greater the pyramidalization angle,  $\theta$  (or out-of-plane angle). For instance, the pyramidalization angle,  $\theta$ , increases in the order  $15.35$  ( $\text{B}=\text{B}$ )  $<$   $61.45$  ( $\text{Al}=\text{Al}$ )  $<$   $66.85$  ( $\text{Ga}=\text{Ga}$ )  $<$   $70.20$  ( $\text{In}=\text{In}$ )  $<$   $84.24^\circ$  ( $\text{Tl}=\text{Tl}$ ). Likewise, as demonstrated in Figure 4, the trend in  $\text{X}=\text{X}$  bond length in the dimer molecule was calculated to be in the order  $1.692$  ( $\text{B}=\text{B}$ )  $<$   $2.757$  ( $\text{Al}=\text{Al}$ )  $<$   $3.064$  ( $\text{Ga}=\text{Ga}$ )  $<$   $3.433$  ( $\text{In}=\text{In}$ )  $<$   $4.394$  Å ( $\text{Tl}=\text{Tl}$ ), correlating with the atomic size of the main group 13 element X.

**Table 3.** Relative Energies for Singlet and Triplet Group 13 Carbenoids ( $\text{HCMeP}(\text{PhN})_2\text{X}$ ) and for the  $\text{C}_2\text{H}_4$  Addition Process, Reactants ( $\text{HCMeP}(\text{PhN})_2\text{X} + \text{C}_2\text{H}_4$ )  $\rightarrow$  Transition State  $\rightarrow$  Addition Product<sup>a,b</sup>

system	$\Delta E_{\text{st}}^c$ (kcal mol <sup>-1</sup> )	$\angle \text{NXN}$ (deg)	$\Delta E^\ddagger^d$ (kcal mol <sup>-1</sup> )	$\Delta H^e$ (kcal mol <sup>-1</sup> )
X = B	-12.90	111.7	2.938	-48.51
X = Al	16.22	83.56	5.048	-8.483
X = Ga	24.50	82.08	14.61	6.940
X = In	32.48	78.02	28.30	25.70
X = Tl	34.69	73.73	75.18	75.10

<sup>a</sup> All were calculated at the B3LYP/LANL2DZ level of theory. For the B3LYP-optimized structures of the stationary points, see Figure 3. <sup>b</sup> Energies differences have been zero-point corrected. See the text. <sup>c</sup> Energy relative to the corresponding singlet state. A positive value means the singlet is the ground state. <sup>d</sup> The activation energy of the transition state, relative to the corresponding reactants. <sup>e</sup> The reaction enthalpy of the product, relative to the corresponding reactants.



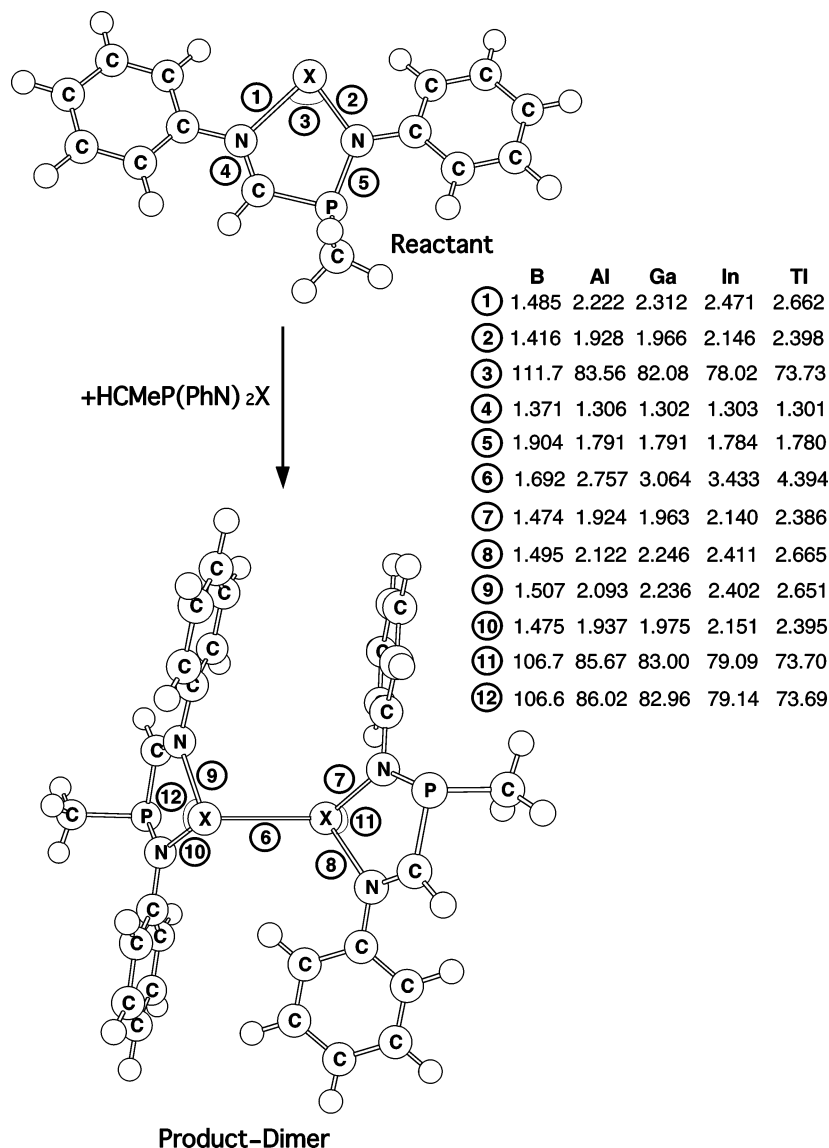


**Figure 4.** B3LYP/LANL2DZ-optimized geometries (in Å and deg) of the reactants (singlet) and dimer products of  $\text{HCMeP}(\text{PhN})_2\text{X}$  ( $\text{X} = \text{B}, \text{Al}, \text{Ga}, \text{In},$  and  $\text{Tl}$ ). The relative energies for each species are given in Table 4. Hydrogens are omitted for clarity. For more information see the text.

**Table 4.** Relative Energies for Singlet and Triplet Group 13 Carbenoids ( $\text{HCMeP}(\text{PhN})_2\text{X}$ ) and for the Dimerization Process, Reactants ( $2\text{HCMeP}(\text{PhN})_2\text{X} \rightarrow \text{Dimerization Product}^{a,b}$

system	$\Delta E_{\text{st}}^c$ (kcal mol <sup>-1</sup> )	$\angle \text{NXN}$ (deg)	$\Delta H^d$ (kcal mol <sup>-1</sup> )	$\Delta G^e$ (kcal mol <sup>-1</sup> )
X = B	-12.90	111.7	-81.82	-63.17
X = Al	16.22	83.56	-11.02	2.208
X = Ga	24.50	82.08	-7.439	4.481
X = In	32.48	78.02	-6.274	4.342
X = Tl	34.69	73.73	-3.722	6.822

<sup>a</sup> All were calculated at the B3LYP/LANL2DZ level of theory. For the B3LYP-optimized structures of the stationary points, see Figure 4. <sup>b</sup> Energies differences have been zero-point corrected. See the text. <sup>c</sup> Energy relative to the corresponding singlet state. A positive value means the singlet is the ground-state. <sup>d</sup> The reaction enthalpy of the product, relative to the corresponding reactants. <sup>e</sup> The Gibbs free energy (298 K) of the product, relative to the corresponding reactants.

In addition, the B3LYP calculations show that the energy of the final products (dimers) relative to their corresponding reactants are -81.82 (B=B), -11.02 (Al=Al), -7.439 (Ga=Ga), -6.274 (In=In), and -3.722 (Tl=Tl) kcal/mol. Also, we have calculated the free energy differences ( $\Delta G$ ) for eq

3 at 298 K, which are also given in Table 4. As shown there, the values of  $\Delta G$  between reactants and dimer are -63.17, +2.208, +4.481, +4.342, and +6.822 kcal/mol for boron, aluminum, gallium, indium, and thallium, respectively. Consequently, our computational results predict that boron derivatives with B=B-bonded dimeric structures are both kinetically and thermodynamically stable with respect to dissociation. In contrast to the boron compounds, the theoretical results demonstrate that, after consideration of the thermodynamic factors, the total energies of the remaining double-bonded dimers are still above that of two separated monomers ( $\text{HCMeP}(\text{PhN})_2\text{X}$ ). The theoretical findings therefore suggest that the dimerization reaction should not occur during the formation of the neutral five-membered  $\text{HCMeP}(\text{PhN})_2\text{X}$  ( $\text{X} = \text{Al}, \text{Ga}, \text{In},$  and  $\text{Tl}$ ) species.

#### IV. Conclusion

In this work, we have studied the mechanisms of three kinds of chemical reactions of neutral five-membered  $\text{HCMeP}(\text{PhN})_2\text{X}$  species by density functional methods. It

should be pointed out that this study has provided the first theoretical demonstration of the reaction trajectory and theoretical estimation of the activation energy and reaction enthalpy for these chemical processes.

Our present theoretical investigations demonstrate that the chemical reactivity of boron, aluminum, gallium, indium, and thallium decrease in the order  $B > Al > Ga > In > Tl$ . From another point of view, our theoretical findings confirm a general belief that one of the important influences on the isolability of a group 13 carbenoid is its group 13 atom center.<sup>1–4</sup> That is to say, our theoretical works strongly imply that, compared with the  $HC(CMeNPh)_2B$  species which is highly reactive, the other neutral five-membered group 13 carbenoids ( $X = Al, Ga, In, \text{ and } Tl$ ) should be stable and readily synthesized and isolated at room temperature.

Regardless of which chemical reaction is considered, it was found that a knowledge of the singlet–triplet splitting of the neutral five-membered  $HCM_eP(PhN)_2X$  molecule is of great importance in understanding its reactivity because it can affect the driving force for chemical reaction. Qualitatively, a greater  $\angle NXN$  bond angle results in a smaller  $\Delta E_{st}$ , a lower the activation barrier, and, in turn, more rapid chemical reactions with various chemical species. Specifically speaking, electronic, as well as steric factors, should play an important role in determining the chemical reactivity

of the neutral five-membered group 13 carbenoids from both kinetic and thermodynamic viewpoints.

Furthermore, we have demonstrated that the computational results can be rationalized using a simple CM model. Although the relative reactivity of various chemical species is determined by the entire potential energy surface, the concepts of the CM model, focusing on the singlet–triplet splitting in the reactants, allows one to assess quickly the relative reactivity of a variety of neutral five-membered group 13 carbenoids without specific knowledge of the actual energies of the interactions involved.

We encourage experimentalists to carry out further experiments to confirm our predictions.

**Acknowledgment.** The authors are grateful to the National Center for High-Performance Computing of Taiwan for generous amounts of computing time. They also thank the National Science Council of Taiwan for the financial support. Special thanks are also due to Referee B and Referee D for very helpful suggestions and comments.

**Supporting Information Available:** Details of the computational approach, relative energies of the compounds, and Cartesian coordinates. This material is available free of charge via the Internet at <http://pubs.acs.org>.

IC0608593